NANO · MICRO small
www.small-journal.com

Appreciating the First Line of the Human Innate Immune Defense: A Strategy to Model and Alleviate the Neutrophil Elastase-Mediated Attack toward Bioactivated Biomaterials

*Carina Blum, Mehmet Berat Taskin, Junwen Shan, Tatjana Schilling, Katrin Schlegelmilch, Jörg Teßmar, and Jürgen Groll**

Biointerface engineering is a wide-spread strategy to improve the healing process and subsequent tissue integration of biomaterials. Especially the integration of specific peptides is one promising strategy to promote the regenerative capacity of implants and 3D scaffolds. In vivo, these tailored interfaces are, however, first confronted with the innate immune response. Neutrophils are cells with pronounced proteolytic potential and the first recruited immune cells at the implant site; nonetheless, they have so far been underappreciated in the design of biomaterial interfaces. Herein, an in vitro approach is introduced to model and analyze the neutrophil interaction with bioactivated materials at the example of nano-bioinspired electrospun surfaces that reveals the vulnerability of a given biointerface design to the contact with neutrophils. A sacrificial, transient hydrogel coating that demonstrates optimal protection for peptide-modified surfaces and thus alleviates the immediate cleavage by neutrophil elastase is further introduced.

1. Introduction

Biointerface engineering aims to foster tissue healing by regulating and tailoring stem cell remodeling processes.[1] Such interfaces are often fabricated by using synthetic polymers, which are inherently bioinert thus has to be further bioactivated for desired applications, e.g., cell adhesion and differentiation processes.[2] In addition to biomaterial surface functionalization, an innovative biomaterial should also imitate hierarchical structures in the body, such as the extracellular matrix (ECM). Thus, biomaterials should interact with the surrounding cells to build up and regenerate tissue.[3] Electrospinning of polymeric fiber meshes is a suitable tool to combine both surface functionalization and structural composition, resulting in an ECM-mimetic material for many applications in tissue engineering and regenerative medicine.[4] In detail, solution electrospinning (ES) easily enables the specific surface bioactivation of fibrous biomaterials,[5] e.g., with cell-mediating peptide sequences like RGD to trigger cell adhesion through exclusive recognition of the immobilized binding motifs.[6] Beyond peptides, whole proteins and/or even decellularized ECMs are often used to closer mimic the complexity of ECM within a functional material.[7] Significant research effort has been dedicated to the development of increasingly complex biomimetic cell-material constructs, with the biological focus on tissue-resident cells.[8]

However, the implantation of a biomaterial always initiates an inevitable immune response reflecting the first step of any innate tissue repair and regeneration.[9] The outcome of this response determines whether the biomaterial will be integrated into the host tissue, leading to proper healing, or it will be encapsulated, rejected, and thus finally fail to fulfill its desired function.[9–10] During the acute inflammatory phase, different cells of the innate immune system consecutively arrive at the biomaterial interface. Amongst those cells, blood originating neutrophils and monocytes as well as monocyte-derived and tissue-resident macrophages, are the most important players.[11] For a long, the interaction of those cells with advanced ECM-mimetic biomaterial constructs has been underappreciated. This has recently become a more active area of research, so far, with a focus on the response of macrophages and their biomaterial-mediated reaction.[10] Prior to the macrophage response, neutrophils are the first immune cells getting into direct contact with the biomaterial construct. However, especially their immune response has been mostly neglected and thus has to be analyzed in more detail.

In an acute inflammatory state, neutrophils remain present in the wound site for up to 72 h. They are continuously replenished and activated, leading to a persistently inflammatory wound environment.[12] Moreover, neutrophils produce and store antimicrobial proteases in cytoplasmic granules, i.e.,

Dr. C. Blum, Dr. M. B. Taskin, J. Shan, Dr. T. Schilling,
Dr. K. Schlegelmilch, Dr. J. Teßmar, Prof. J. Groll
Department of Functional Materials in Medicine and Dentistry at the Institute of Functional Materials and Biofabrication (IFB)
University of Würzburg and KeyLab Polymers for Medicine of the Bavarian Polymer Institute (BPI)
Pleicherwall 2, Würzburg 97070, Germany
E-mail: juergen.groll@fmz.uni-wuerzburg.de

The ORCID identification number(s) for the author(s) of this article can be found under https://doi.org/10.1002/smll.202007551.

DOI: 10.1002/smll.202007551

neutrophil elastase (NE), cathepsin G, and protease 3, which can be readily released into the extracellular space upon activation mainly to kill and degrade microbes during inflammation. Nevertheless, these proteases also cleave components of the basement membrane and the ECM of the surrounding tissue such as elastin,[13] fibronectin,[13a,14] laminin,[13a,15] and collagen[13,16] usually to ensure the effective removal of injured tissue during a dynamic developmental process and tissue remodeling.[17] Considering the described immense capacity of neutrophils to recognize and degrade foreign body material such as surface-immobilized bioactive molecules, it is advisable to design the biomaterial to resists the neutrophil attack undamaged.

In general, biomaterial engraftment is always accompanied by tissue injury with an immediate host response, followed by the invasion of resident stem cells and tissue cells, which cause tissue remodeling. Our study design exactly connects the immediate immune reaction and the subsequent tissue regeneration. Therefore, we pioneer a simplified but robust in vitro model to analyze neutrophil´s cleavage potential toward immobilized peptide moieties onto a nanofibrous material, and subsequent human mesenchymal stromal cell (hMSC) adhesion was used as a readout tool to evaluate neutrophil´s cleavage potential. In detail, to assess the cleavage potential of in vitro-derived human neutrophil elastase (HNE), an RGDS-containing peptide with an HNE-specific cleavage site is immobilized on the surface of poly(ε-caprolactone) (PCL) nanofibers using an ultrathin hydrophilic surface coating. Accordingly, the peptide integrated the AAPV-motif to allow for specific peptide cleavage by HNE and the cell-mediating RGDS-motif for subsequent hMSC adhesion. Thus, we confirmed the main hypothesis of HNE cleavage function with cell adhesion tests. The degradation of peptide function directly at the HNE-specific cleavage site led to removed cell-mediated RGDS-motifs with subsequently reduced cell adhesion. However, the neutrophil-mediated peptide degradation is an undesirable response, so we extended our model system by embedding the biomaterial in a temporary protective hydrogel during the neutrophil elastase-mediated attack to prevent neutrophil-mediated peptide degradation. The transient hydrogel coating blocked the neutrophil-specific cleavage site and was subsequently dissolvable within 5 days. Thus, we successfully confirmed the preservation of fiber surface bioactivity during the neutrophil elastase-mediated attack since the subsequent cell adhesion was no longer reduced.

2. Results and Discussion

2.1. Fabrication of Peptide-Bioinspired PCL Fiber Meshes

We have developed an in vitro proof-of-principle model to imitate the cleavage potential of neutrophil elastase toward a polymeric, nanofibrous biomaterial with covalently immobilized peptide functions (**Scheme 1**). A customized peptide sequence with an integrated specific human neutrophil elastase (HNE-) cleavage site (AAPV-motif) was covalently immobilized to a poly(ε-caprolactone) (PCL) fibrous mesh.

In general, electrospinning can be applied to manufacture biomedical materials such as medical implants, antimicrobial materials, wound dressings, drug delivery vehicles, and enzyme immobilized membranes.[18] Furthermore, electrospun fibers have been extensively investigated for tissue engineering applications, including cartilage,[19] skin,[20] and stem cell-engineering[21] approaches. A major challenge to control the biological behavior of cells and how a biomaterial interacts with the body is the proper surface functionalization of nanofibrous meshes. To achieve specific cell adhesion, fibers' surface might be modified post-spinning, for instance, by coating of the mesh with a solution of biological additives.[22] Another, more straightforward route of functionalization for solution electrospun fibers adds biological molecules directly into the spinning solution prior to processing.[4b] Electrospinning of polyesters with the six-arm star-shaped prepolymer NCO-sP(EO-*stat*-PO) as reactive and amphiphilic additive allows for the fabrication of fibers with an ultrathin hydrophilic surface coating that suppresses non-specific protein adsorption and therefore non-specific cell adhesion.[4b,5,23] Thereby, this non-fouling characteristic of the hydrophilic fibers serves a prerequisite for introducing any targeted, i.e., cell-specific modification. First of all, we verified the repellent properties of the PCL/NCO-sP(EO-*stat*-PO) meshes by incubation with texas red-labeled bovine serum albumin (TRBSA) as a model protein (Figure S1, Supporting Information). While these NCO-sP(EO-*stat*-PO)-modified meshes showed almost no fluorescence for TRBSA, indicating the expected prevention of protein adsorption, pure PCL meshes demonstrated a strong fluorescence signal and hence BSA adsorption. Accordingly, Salber et al. (2007) described the prevention of non-specific cell adhesion on a plasma-activated PDMS substrate due to a coating with a star-shaped

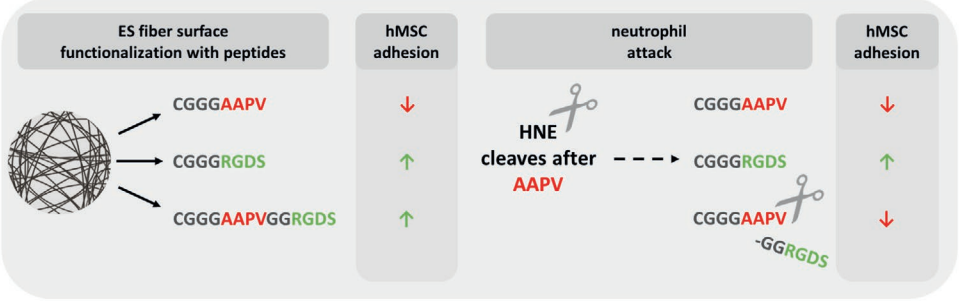

Scheme 1. Schematic presentation of solution electrospun fiber functionalization and peptide-cleaving activity of human neutrophil elastase (HNE) with subsequent hMSC adhesion as readout. Solution electrospun PCL/NCO-sP(EO-*stat*-PO) fibers are covalently functionalized with three peptides (CGGGAAPV, CGGGRGDS, and CGGGAAPVGGRGDS). Human neutrophil elastase (HNE) cleaves the covalently immobilized CGGGAAPVGGRGDS peptide at the C-terminus of the specific cleavage sequence AAPV resulting in the elimination of the GGRGDS sequence.

isocyanate-terminated prepolymer.[23] For the introduction of targeted modifications mentioned above though the reactive isocyanate groups of the NCO-sP(EO-*stat*-PO) additive can be further used as a covalent linker to modify the fiber surface resulting in an ultrathin coating with bioactive molecules that contain reactive groups such as thiols (–SH), amines ($–NH_2$), or hydroxyl (–OH) groups. This strategy enables a selective and specific cell adhesion onto the fibrous mesh due to the covalent attachment of cell adhesion-mediating peptides (i.e., RGD-motif) to the hydrophilic fiber surface.[5a,24] Thus, in the present study, we intended to covalently attach specific ligands with a terminal RGDS-motif to PCL/NCO-sP(EO-*stat*-PO) meshes to enable distinct interactions of human mesenchymal stromal cells (hMSCs) with the otherwise inert surfaces. Therefore, peptide sequences (CGGGAAPV, CGGGRGDS, and CGGGAAPVGGRGDS) were added into the electrospinning solution, and scanning electron microscopy (SEM) analysis showed that the peptides did not influence fiber morphology and diameter of the resulting meshes (Figure S2, Supporting Information). The detected structural properties of the non-woven (peptide-modified) PCL/NCO-sP(EO-*stat*-PO) nanofiber meshes, i.e., their high porosity, high pore interconnectivity, and high surface to volume ratio, are typical for solution electrospun meshes.[25]

In detail, we have designed a selective peptide sequence with a terminal cell-binding RGDS-motif and a specific HNE cleavage sequence (AAPV-motif)[26] in the middle of the peptide with glycine (G) residues as spacer to the cysteine (C) binding site. According to the literature, the HNE enzyme is supposed to cleave the designed peptide at the C-terminus of AAPV, resulting in the elimination and release of the GGRGDS cell-binding residue into the aqueous solution (Scheme 1).

2.2. Quantification of HNE Cleavage Potential toward Covalently Immobilized Peptides onto PCL Fiber Meshes

Within this study, we aimed to imitate neutrophil´s elastase-mediated cleavage potential by incubation of our peptide-modified non-wovens with in vitro-derived HNE obtained from isolated, PMA-stimulated human neutrophils (Figure S3, Supporting Information) in HBSS, while for the control pure HBSS was used. As commercially available HNE-specific peptide substrates contain the AAPV sequence terminally conjugated with a fluorogenic or chromogenic (e.g., *para*-nitroaniline (*p*NA)) motif, the general cleavage capacity of the HNE enzyme toward our self-designed AAPV-containing substrate was tested using the chromogenic CGAAPV-*p*NA substrate. The release of *p*NA upon cleavage by in vitro-derived HNE increased continuously over time (Figure S4, Supporting Information). Hence, we confirmed the activity of our in vitro-derived HNE by the cleavage of the CGAAPV-*p*NA substrate in aqueous solution in accordance with the literature.[27]

Having successfully proven the AAPV cleavage site for HNE in an aqueous solution, we aimed to use this motif within a covalently immobilized peptide for its release by HNE from the polymeric backbone of a biomaterial. Therefore, we exploited the solution electrospinning method to prepare peptide-functionalized meshes based on PCL to explore their suitability for future in vivo applications.

The linkage of bioactive peptide sequences in our model to the fiber surface is essential for improving their performance and function. Since it is challenging to quantify the presence and the amount of short peptide sequences on biomaterial surfaces, we previously developed a novel, convenient technique to measure quantitatively small amounts of peptide sequences linked to fibrous meshes. Briefly, the cleavable, UV-sensitive 2-mercaptopyridine, was linked as a reactive group to the HNE-sensitive RGD-modified peptide via disulfide formation with the thiol group of cysteine. Addition of *tris*(2-carboxyethyl) phosphine (TCEP) into the solution reduced the disulfide bridge and thereby released the functional 2-mercaptopyridine groups entirely (Figure S5, Supporting Information). The 2-mercaptopyridine quantification procedure was used as a readout tool for HNE-cleaved peptide but had to be divided into several steps to discriminate between peptide amounts attached via different binding modes and to allow for the evaluation of the actual HNE effect (**Scheme 2**). Based on the measured UV absorbance for 2-mercaptopyridine, ≈90% of the peptide input were retrieved and either detected on the fiber surface (60% physically adsorbed and 20% covalently bound) or embedded in the PCL fiber (5%) (**Figure 1**). After washing off the physically adsorbed peptides, the meshes were incubated in in vitro-derived HNE for 24 h leading to the enzymatic cleavage of almost all covalently bound peptides on the fiber surface. Only ≈3% of labeled peptide remained covalently bound onto the fiber. Thus, the cleavage potential of HNE toward the covalently bound model peptide at the integrated HNE cleavage site (AAPV) was confirmed.

2.3. Model Peptide Cleavage by In Vitro-Derived HNE Decreases Human Mesenchymal Stromal Cell (hMSC) Adhesion

We mimicked the neutrophil attack in our model by incubating the peptide-functionalized non-woven with in vitro-derived HNE for 24 h at 37 °C resembling body temperature. The time interval of 24 h was chosen according to the in vivo conditions, since it was originally assumed that neutrophils survive in tissue for a maximum of 24 h.[12b] In addition, also other in vitro studies imitate the neutrophil attack by incubation with HNE for 24 h at 37 °C.[28] The surface morphology of the PCL/NCO-sP(EO-*stat*-PO) fibrous meshes functionalized with control CGGGRGDS or HNE-specific CGGGAAPVGGRGDS peptide was not altered through this simulated neutrophil elastase-mediated attack (Figure S6, Supporting Information).

For the intended application as a proof-of-principle method, we analyzed cell attachment on our non-wovens to evaluate the HNE cleavage capacity. Therefore, we promoted hMSC adhesion by immobilizing the RGDS-based cell-mediating peptide to the PCL/NCO-sP(EO-*stat*-PO) mesh. More precisely, meshes functionalized with CGGGAAPVGGRGDS peptide were investigated regarding hMSC adhesion after HNE cleavage at the C-terminus of the sequence AAPV (Scheme 1B). In general, the RGD-motif derived from fibronectin in the ECM is well-known to mediate cell adhesion on synthetic materials.[29] Accordingly, Shao et al. (2012) proved the adhesion of bone-marrow derived MSCs on RGD-conjugated PCL electrospun meshes with excellent cell spreading and proliferation.[30] Moreover, the

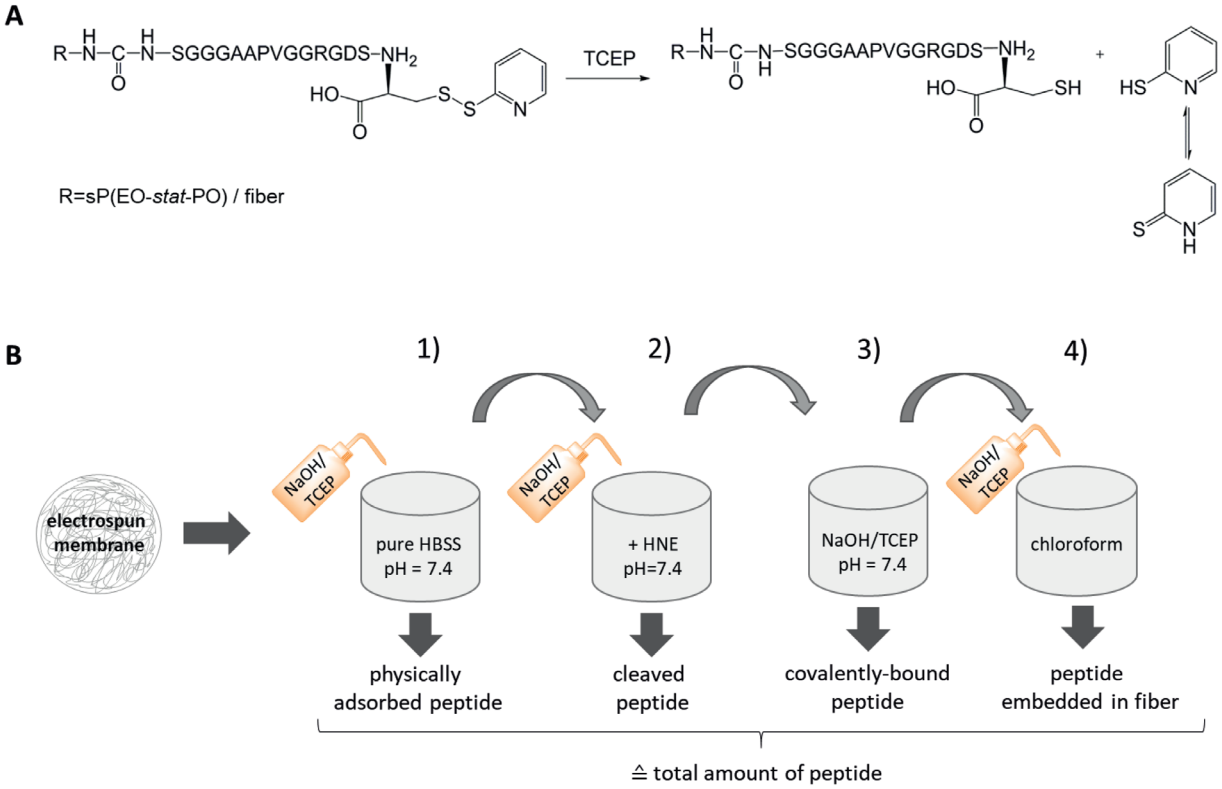

Scheme 2. Workflow for the quantification of peptides associated with the fiber mesh (according to their binding mode). A) The disulfide bridge within the modified peptide is cleaved by TCEP and the released amount of 2-mercaptopyridine is detectable with UV spectroscopy. B) To quantify the total amount of modified peptides associated with the meshes, these had to be treated in four consecutive steps, which allowed for the distinction and retrieval of peptide amounts attached via different binding modes. After each treatment, the concentration of 2-mercaptopyridine proportionally released from the modified model peptide was determined UV-metrically by correlation to a standard curve of the peptide. 1) Meshes were incubated in pure HBSS buffer to wash off physically adsorbed peptides. The supernatants were freeze-dried and the lyophilisates were dissolved with NaOH/TCEP solution. 2) To analyze the amount of peptide that was degradable by HNE, the meshes were treated with in vitro-derived HNE (+HNE) for 24 h at 37 °C. The supernatants, containing peptides detached from the meshes by HNE, were freeze-dried and dissolved with NaOH/TCEP solution. 3) To quantify residual, still covalently attached peptides, these were removed by incubation with NaOH/TCEP solution and the concentration of 2-mercaptopyridine was directly determined in the supernatant. 4) Peptides embedded within the fibers were quantified by dissolving the mesh in chloroform. The solvent was removed and the precipitate was dissolved in NaOH/TCEP solution prior to 2-mercaptopyridine determination.

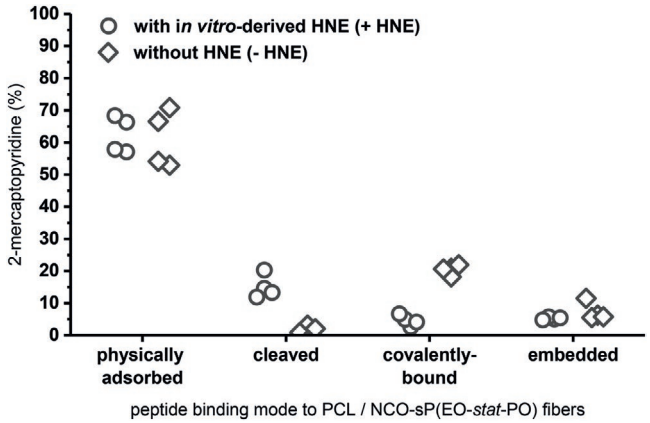

Figure 1. Quantification of RGDS-modified peptide on the surface of electrospun fibers via 2-mercaptopyridine release. The release of 2-mercaptopyridine was detected after each single step by incubating with the cleaving agent *tris*(2-carboxy-ethyl) phosphine (TCEP). Around 20% of the modified peptide was covalently bound, and almost 75% of the covalently bound peptide amount was cleaved by in vitro-derived HNE (+ HNE) applied after the removal of physically adsorbed peptides ($n = 4$).

RGD-motif also improves adhesion, spreading, and proliferation of L929 fibroblasts, as has been shown by Karakecili et al. (2007) on chitosan membranes.[31]

Cell adhesion and activity on PCL/NCO-sP(EO-*stat*-PO)/CGGGAAPVGGRGDS meshes after incubation with in vitro-derived HNE was evaluated and compared to five controls: i) tissue culture polystyrene (TCPS), PCL/NCO-sP(EO-*stat*-PO) meshes ii) without peptide, with immobilized iii) CGGGAAPV, iv) CGGGRGDS, and v) CGGGAAPVGGRGDS peptide not treated with HNE. While only low cell adhesion and activity were observed on the reference PCL/NCO-sP(EO-*stat*-PO) meshes without and with immobilized CGGGAAPV peptide, hMSC cell attachment was markedly increased in the presence of immobilized peptides with RGDS-motif (**Figure 2**). Here, 64.8±6.0% and 56.2±5.9% hMSCs attached to PCL/NCO-sP(EO-*stat*-PO) meshes with immobilized CGGGAAPVGGRGDS and CGGGRGDS, respectively, compared to TCPS. In contrast, cell attachment significantly declined down to ≈14% on CGGGAAPVGGRGDS-meshes after incubation with in vitro-derived HNE, which cleaved the peptide and hence removed the RGDS motif. The specificity of this

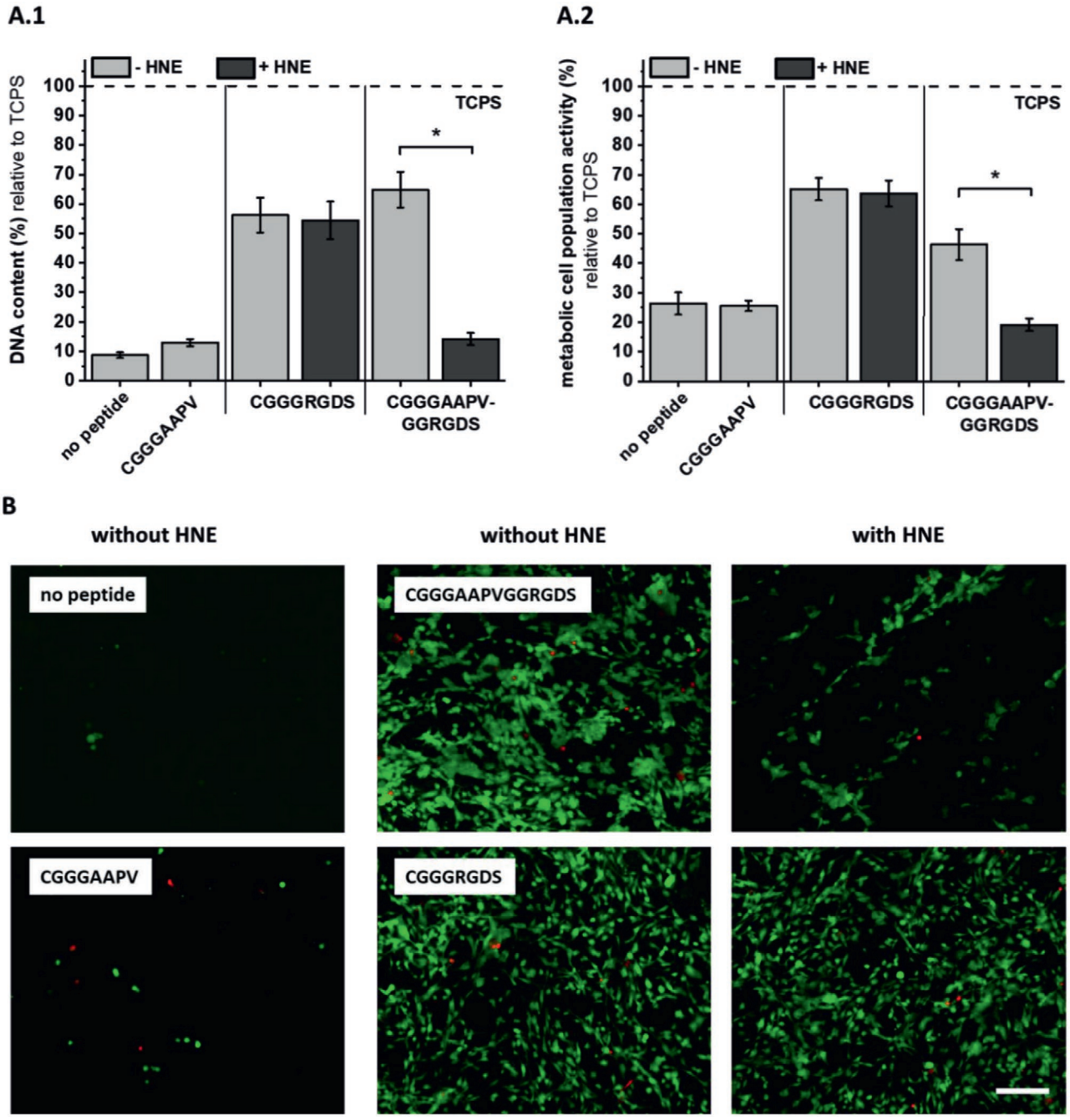

Figure 2. hMSC cell adhesion on peptide-decorated meshes after incubation with or without in vitro-derived HNE. DNA content (A.1) and metabolic cell population activity (A.2) on PCL/NCO-sP(EO-*stat*-PO) meshes functionalized with CGGGAAPVGGRGDS, CGGGRGDS, CGGGAAPV, and without immobilized peptide, respectively, that were incubated with (+) or without (–) HNE at 37 °C for 24 h, prior to cell seeding. Both assays were performed on day 1 after cell seeding and the data are normalized to tissue culture polystyrene (TCPS) set to 100%. ($N = 3$, $n = 3$). *$p < 0.05$. B) Corresponding live/dead staining for the visualization of hMSC adhesion (viable cells: green, dead cells: red). Cell adhesion decreased on PCL/NCO-sP(EO-*stat*-PO)/CGGGAAPVGGRGDS after incubation with HNE. Scale bar = 200 µm.

simulated elastase-mediated neutrophil attack was confirmed, as hMSC adhesion on CGGGRGDS-conjugated meshes, i.e., without integrated AAPV-motif, was not affected by HNE addition. In accordance, live/dead (Figure 2B) and SEM imaging (Figure S7, Supporting Information) showed similar amounts of viable cells on PCL/NCO-sP(EO-*stat*-PO) meshes with immobilized CGGGRGDS after incubation with or without HNE and with immobilized CGGGAAPVGGRGDS without HNE incubation. Cell adhesion was significantly reduced on CGGGAAPVGGRGDS-conjugated meshes after the simulated neutrophil attack (addition of in vitro-derived HNE). Only a few cells adhered on PCL/NCO-sP(EO-*stat*-PO) and

PCL/NCO-sP(EO-*stat*-PO)/CGGGAAPV fibers due to their protein repellent properties[5a] and missing cell-adhesion motifs,[6] respectively (Figure 2). The hydrophilicity of PCL/NCO-sP(EO-*stat*-PO) fibers fundamentally prevents proteins from the medium as well as cellular proteins secreted and produced by the hMSCs to be adsorbed onto the fibers, which inhibits subsequent cell adhesion. In accordance, Grafahrend et al. (2010) also showed the suppression of non-specific protein adsorption and, therefore, reduced cell adhesion on solution electrospun fibers based on poly(lactide-*co*-glycolide) (PLGA) and the functional NCO-sP(EO-*stat*-PO) additive.[4b] In our study, the missing cell adhesion on PCL/NCO-sP(EO-*stat*-PO)/CGGGAAPV fibers demonstrated that the attachment of a non-RGDS-containing peptide sequence onto the fiber surface maintains its ability to resist non-specific cell adhesion.

Concluding, the quantification experiment (Figure 1) that confirmed the highly efficient cleavage of covalently bound AAPV-modified peptides by HNE together with the cell adhesion study (Figure 2) proves that the decreased hMSC adhesion on HNE-treated CGGGAAPVGGRGDS-conjugated meshes arise due to the enzymatic abolishment of the RGDS-motif.

2.4. Hydrogel Coating Protects Biomimetic Fiber Functionalization against Cleavage by Neutrophil Elastase

With our newly established model, we were able to confirm the cleavage capacity of HNE toward covalently immobilized peptides on a polymeric matrix. However, for an in vivo application of a peptide-conjugated biomaterial, e.g., for providing adhesion or differentiation stimuli for stem cells during tissue renewal, it is essential to ensure the integrity of the biomaterial and its bioactive cues. Therefore, we investigated a hydrogel coating, which is soluble within a few days under body-like conditions, for its protective effect on the functionalized meshes against the simulated neutrophil elastase-mediated attack (**Figure 3**).

In the context of wound healing so far, hydrogels have mainly been used as wound dressings to ameliorate the healing process and to protect the site of injury from infections.[32] In our study, a hydrogel, as part of a composite biomaterial, is used as a sacrificial protective layer, which has the property to dissolve under hypotonic conditions and, thus, exposes the bio-functionality of the embedded non-woven for subsequent cell responses.

The hydrogel coating was formed via Schiff Base chemistry of an aldehyde group within primary oxidized hyaluronic acid (proxHA) with an amine derivate using adipic acid dihydrazide (ADH) following elimination of water to form the final imine derivate.[33] Ideally, the hydrogel coating preserves the peptide modification from being cleaved by the HNE enzyme during the initial neutrophil attack upon implantation, as shown by our experiments without protective means (Figure 2).

Therefore, we first analyzed the HNE diffusion limit through proxHA hydrogels via CGAAPV-*p*NA peptide cleavage after HNE diffusion (**Figure 4**A). The enzyme was efficiently excluded within the first 5 h of exposition, followed by a slow and continuous rise over the next hours/days. Only ≈13.0% of CGAAPV-*p*NA molecules were cleaved by HNE that diffused through the proxHA hydrogel after incubation for 24 h. Thereby, the duration of 24 h exactly reflects the time used to imitate the neutrophil attack by HNE in our self-developed model system with the subsequent cell adhesion experiments.

We intended to use the proxHA hydrogel for protecting the RGDS-containing peptide sequence of our bioactivated PCL fibers from being cleaved by HNE. Throughout the HNE incubation and hydrogel dissolution steps, we used a hypotonic buffer system based on equivalent volumes of HBSS and distilled water. It is well-known that the Schiff Base chemistry is reversible in water with a constant equilibrium of free and bound polymer chains leading to permanent loss of polymer chains.[33] Therefore, it was assumed that the hydrogel would also swell and dissolve under hypotonic conditions, albeit over a more extended time period compared to pure water.

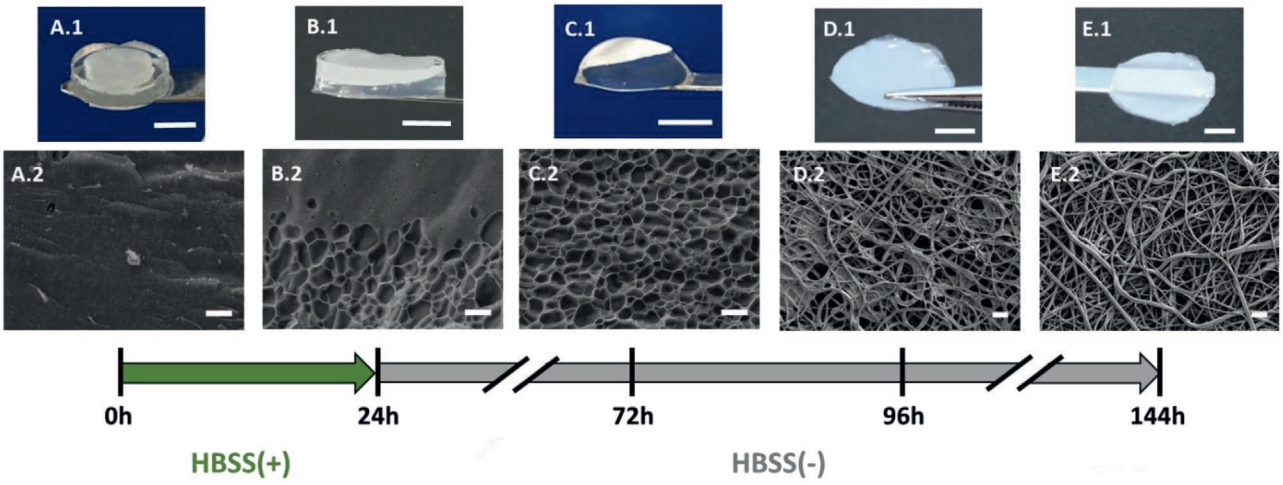

Figure 3. Time profile for the uncovering of the solution electrospun mesh after dissolution of the surrounding and protecting hydrogel. Composites are incubated in HBSS buffer, initially supplemented with in vitro-derived HNE (HBSS+). Upper row: Photographs of the composite biomaterial: PCL/NCO-sP(EO-*stat*-PO)/CGGGAAPVGGRGDS mesh embedded within proxHA (primary oxidized hyaluronic acid) hydrogel. Lower row: Cryo-SEM (A-C) and SEM (D, E) images of the hydrogel dissolution behavior over time with increasing hydrogel porosity and visibility of the fiber morphology of the uncovered solution electrospun mesh, respectively. Scale bar: 6 mm (upper row), 5 µm (lower row).

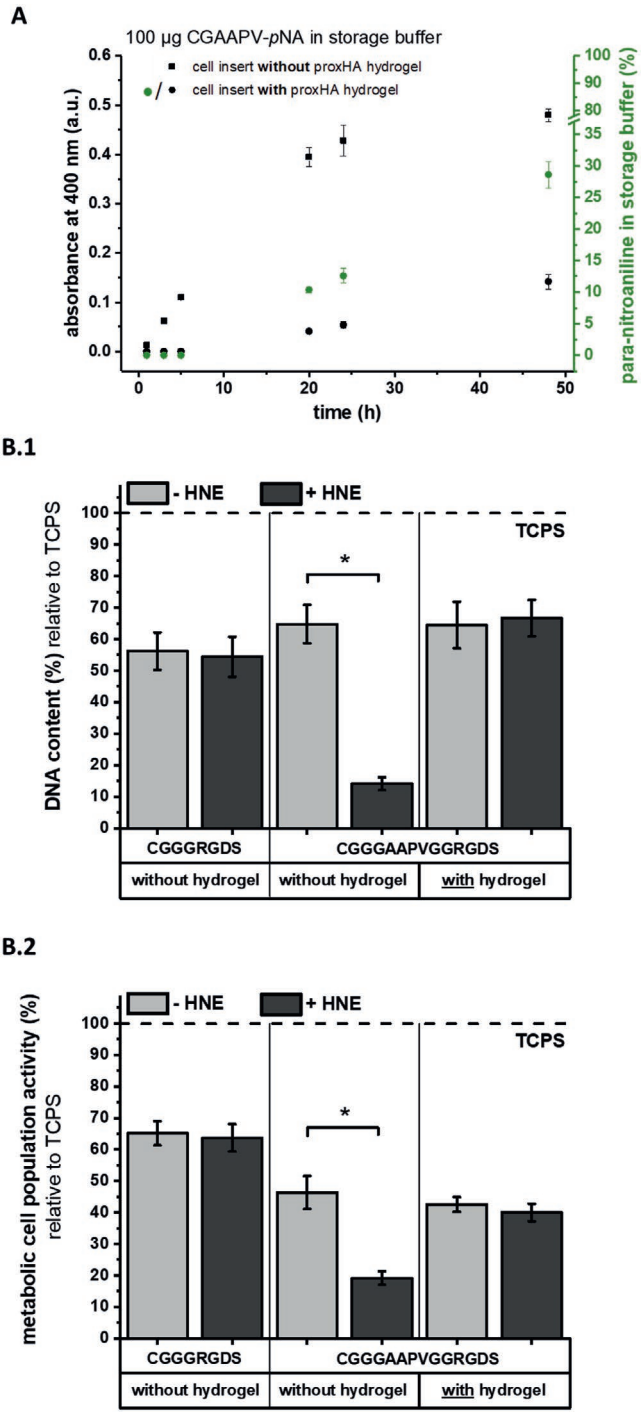

Figure 4. Limited diffusion of HNE through 3% w/w proxHA hydrogel. A) CGAAPV-*p*NA diluted in pure HBSS was stored in the lower compartment of a transwell system (= storage solution), while the hydrogel was placed into a cell insert with HNE (+ HNE) or without HNE (- HNE) on top. The release of *p*NA in the storage solution after diffusion of HNE through the hydrogel was determined after certain time points at 400 nm ($n = 4$). After 24 h incubation with HNE, only ≈13% of *p*NA molecules were determined in the lower compartment after HNE diffusion through the hydrogel and subsequent peptide cleavage. DNA content (B.1) and metabolic cell population activity (B.2) of hMSCs at day 1 on PCL/NCO-sP(EO-*stat*-PO)/CGGGRGDS meshes without hydrogel protection and PCL/NCO-sP(EO-*stat*-PO)/CGGGAAPVGGRGDS meshes with or without surrounding hydrogel during HNE treatment. Composites were incubated with (+) or without (–) HNE at 37 °C for 24 h, prior to dissolving the hydrogel in pure HBSS for 5 days. The data are normalized to tissue culture treated polystyrene (TCPS) set to 100% (without hydrogel: $N = 3$, $n = 3$; with hydrogel: $N = 1$, $n = 3$) $^*p < 0.05$.

In detail, directly after preparation, the hydrogel exhibited a dense network in the nanometer range (Figure 3; up to 24 h) that swelled within the next two days with increasing porosity (Figure 3; 72 h) and subsequently revealed the embedded solution electrospun mesh (Figure 3; 96 h). Initially, hydrogel residues were still present in the fibrous network, which finally dissolved within the next 2 days (Figure 3; 144 h). Despite of the initial 24 h HNE treatment, the morphology of the bioactivated PCL fibers that were embedded in the proxHA hydrogel was preserved (Figure 3; 120 h). The level of hMSC adhesion on CGGGAAPVGGRGDS-conjugated meshes recovered from the hydrogel constructs was found similar to that of non-embedded meshes that were not treated with HNE and, therefore, suggested a successful protection from enzymatic digestion (Figure 4B).

In addition, SEM and live/dead analysis showed similar number of hMSCs remained attached on the bioactivated, HNE-treated fibers previously embedded in a proxHA hydrogel compared to non-embedded fibers without a neutrophil elastase-mediated attack (Figure S8, Supporting Information). The dissolution behavior of the hydrogel system used in this study, based on aldehyde containing oxidized hyaluronic acid, was adjusted by tonicity of the buffer system. While proxHA hydrogels were long-time stable in isotonic HBSS buffer with gel shrinking within the first hours (Figure S9, Supporting Information), these gels initially swelled and dissolved under hypotonic HBSS conditions within 3–4 days (Figure 3). Although for an in vivo application, the hydrogel system has to be improved regarding its dissolution behavior under body-like conditions, it still proved as a successful in vitro model for the protection from the enzymatic cleavage by neutrophil elastase .

3. Conclusions

In summary, we have presented an in vitro proof-of-principle model to test for the immediate biomaterial interaction with neutrophils as first recruited immune cells upon implantation. The model involves the direct contact of a peptide-decorated nanofibrous biomaterial with human neutrophil elastase (HNE) derived from PMA-stimulated neutrophils resulting in the degradation of the bioinspired material. Consequentially, we advanced the model by embedding the non-woven into a sacrificial, temporary hydrogel coating that protects the peptide-decorated fibers against the neutrophil elastase-mediated attack. The temporary hydrogel coating within this composite biomaterial shows tunable solubility under body-like conditions and protected the peptide-decorated fibrous biomaterial from cleavage by neutrophil elastase . Accordingly, our findings contribute to improving the development and functionality of peptide-based bioinspired materials not only for fibrous structures but also for other formats to increase the success rate of biomaterials and their desired function.

4. Experimental Section

Unless stated otherwise, all reagents were purchased from Sigma-Aldrich (Darmstadt, Germany).

Solution Electrospinning of Surface-Modified PCL-Based Fiber Meshes: The preparation of the electrospinning solution and the spinning process were conducted as described previously via an in-house manufactured electrospinning setup.[4b,22] At first, the peptides CGGGAAPV, CGGGAAPVGGRGDS, and SGGGAAPVGGRGDSC-thiopyridine (all jpt Peptide Technologies GmbH, Berlin, Germany) were dissolved in anhydrous Dimethylformamide (DMF) and added to NCO-sP(EO-*stat*-PO) (DWI Leibniz-Institute for Interactive Materials, Aachen, Germany) for chemical conjugation via NCO groups for 10 min at room temperature (RT) under stirring. Subsequently, the remaining solvent was added to the solution and mixed briefly. Lastly, poly(ε-caprolactone) (PCL, 80 kDa) was added into the blend and mixed for at least 2 h on a magnetic stirrer until a homogenous electrospinning solution was obtained. The final polymer content of the solution was 14.54% PCL and 2.42% NCO-sP(EO-*stat*-PO) w/v, dissolved in anhydrous DCM:DMF(7:4) v/v mixture. Briefly, the polymer solution was transferred into a 1 mL syringe and mounted into a syringe pump. The syringe was capped with a stainless steel needle (27G) and a voltage of 10 kV was applied. The polymer fibers were collected onto a grounded, rotating (≈100 rpm) metallic mandrel (diameter 60 mm, length 100 mm), placed 15 cm away from the needle. The feeding rate of the solution was set to 0.5 mL h^{-1}. The meshes were freeze-dried for 1 day to remove the remaining solvents prior to cutting the meshes into small, round pieces (Ø = 9 mm).

Isolation of Human Neutrophils and Preparation of In Vitro-Derived Human Neutrophil Elastase (HNE): All experiments were performed with the approval of the Local Ethics Committee of the University of Würzburg. Peripheral blood from human adult volunteers was obtained with the written informed consent of each blood donor. Citrate-dextrose solution (ACD) was used as an anticoagulant during blood collection. Neutrophils were isolated by density gradient centrifugation with low-density Pancoll (Density: 1.077 g L^{-1}; Pan-Biotech, Aidenbach, Germany) as described elsewhere.[34] In detail, blood was mixed with an equivalent volume of 3% w/v dextran (MW 150.000 g mol^{-1}) in 0.9% NaCl and incubated at room temperature for 20 min. The emerged upper layer containing neutrophils was transferred onto low-density Pancoll and centrifuged at 400xg for 30 min. To lyse the remaining red blood cells, the neutrophil/erythrocyte pellet was resuspended in ice-cold 0.2% NaCl, incubated for 30 s prior to restore isotonicity by adding ice-cold 1.6% NaCl. The suspension was centrifuged at 300xg for 6 min, and the lysing steps were performed in total for three times. Subsequently, the neutrophil pellet was resuspended in HBSS, and 1×10^6 cells were cultivated in non-treated 24-well plates (Corning, Corning (USA)) in a humidified atmosphere at 37 °C and 5% CO_2 for 1 h to allow cell seeding. Afterward, phorbol 12-myristate 13-acetate (PMA) was added to the neutrophils at a final concentration of 100 ng PMA mL^{-1}, and the neutrophil-PMA preparation was incubated at 37 °C for 1 h without CO_2. The supernatant was centrifuged at 40.000 *g* for 15 min to obtain soluble products from in vitro-derived HNE from PMA-stimulated neutrophils and stored at −80 °C until use. The activity of in vitro-derived HNE was measured using the neutrophil elastase activity kit according to the manufacturer's instructions. In brief, the fluorescence signals of standards and samples were measured in a kinetic mode for 20 min at 37°C by means of a Tecan Spark 20M plate reader (Tecan, Crailsheim, Germany) at a wavelength of 380/500 nm (excitation/emission). Neutrophil elastase activity was calculated using a standard curve.

Prior to use, elastase activity was adjusted to 2.5 µg HNE in a total volume of 500 µL comprised of equal volumes of HBSS and distilled water (= in vitro-derived HNE (+ HNE)). Accordingly, pure HBSS without HNE (= − HNE) also consisted of equivalent volumes of HBSS and distilled water.

Flow Cytometry: To determine the purity of isolated neutrophils, the surface proteins CD3, CD14, CD15, and CD16b (Milteny Biotec, Bergisch Gladbach (D)) were quantified via flow cytometric analysis on a FACSCalibur device (BD Bioscience, Heidelberg (D)) (Figure S3, Supporting Information). Resuspended neutrophils were incubated with specific antibodies or the corresponding isotype controls, according to the manufacturer's protocol (**Table 1**). After centrifugation at 300xg for 10 min, the supernatant was discarded, and the pellets were resuspended with 500 µL FC-buffer (phosphate-buffered saline (PBS), pH 7.2, 0.5% bovine serum albumin (BSA), 2×10^{-3} M EDTA). Data were analyzed with the Software "FlowJo" (FlowJo LLC, Ashland (USA)). Appropriate cell gating excluded dead cells and cell debris. Additionally, the viability of isolated neutrophils was determined by Flow cytometry using 7-AAD (Milteny Biotec, Bergisch Gladbach (D)).

Table 1. Antibodies for flow cytometry.

Antibody against	Isotype	Fluorescence dye
CD3, human	recombinant human IgG_1	PerCP
CD14, human	mouse IgG_2	FITC
CD15, human	mouse IgM	PE
CD16b, human	recombinant human IgG_1	FITC

Protein Adsorption: Fiber meshes were pre-wetted with deionized water for 60 min, and 500 µL of Texas Red labeled bovine serum albumin (TRBSA; 50 µg mL^{-1} in 1x PBS) were added. After 3 h incubation at RT in the dark, the meshes were washed three times via discarding the solution and refilling the wells (1 mL, 1x PBS) followed by incubation for 20 min in the last washing solution. This procedure was repeated 5 times in total prior to analysis by fluorescence microscopy (Zeiss Axio Imager.M1, Carl Zeiss, Jena, Germany).

Quantification of Immobilized Peptides: For the quantification of immobilized peptides, the UV-detectable group 2-mercaptopyridine (also known as 2-thiopyridine) was linked to the peptide sequence SGGGAAPVGGRGDS via a cysteine disulfide bridge (SGGGAAPVGGRGDSC-2-thipyridine; jpt Peptide Technologies GmbH, Berlin, Germany). The SGGGAAPVGGRGDSC-thiopyridine-modified fiber mesh was prepared in the same way as the common peptide-modified mesh described above. After electrospinning, the meshes were cut into pieces (3 × 6 cm) and weighted. The reducing agent *tris*(2-carboxy-ethyl) phosphine (TCEP) was used to cleave the disulfide bridge within the modified peptide to release the UV-detectable 2-mercaptopyridine into the supernatant, which was measured using the plate reader at 270 nm (Scheme 2A).

The workflow for the quantification of peptides associated with the fiber mesh is shown in Scheme 2B. In detail, the peptide-functionalized fiber meshes were washed in HBSS buffer for 8 h on a shaker to remove physically adsorbed peptides. Afterward, the supernatants were freeze-dried and the lyophilisates were dissolved in NaOH/TCEP solution (3.46×10^{-5} mol mL^{-1} TCEP in 0.1 M NaOH, pH = 7.4) to chemically release 2-mercaptopyridine that could be determined UV-metrically at 270 nm (= physically/non-covalently adsorbed peptides). The meshes were treated with HNE (+ HNE) for 24 h at 37 °C to detach covalently bound peptides accessible for enzymatic cleavage. These supernatants were also freeze-dried and the following steps were performed as described above (= HNE-cleaved, formerly covalently bound peptides). The fiber meshes were directly incubated with NaOH/TCEP solution to remove all residual covalently bound peptides from the fiber surfaces. The emerged supernatants were directly UV-metrically measured to quantify the concentration of 2-mercaptopyridine corresponding to residual, covalently bound peptides on the fibers that were not affected by enzymatic cleavage (= enzymatically non-cleaved, covalently bound peptides). Finally, the meshes were dissolved in chloroform for 2 h, the solvent was removed under high vacuum and the precipitates were dissolved with NaOH/TCEP solution prior to measuring the 2-mercaptopyridine concentration corresponding to peptides embedded in the fibers of the mesh (= embedded peptides). The standard curve was calculated from measuring different known concentrations of the model peptide in NaOH/TCEP solution.

Protection of Bioactive PCL Fiber Meshes by Hydrogels Based on Aldehyde Containing Hyaluronic Acid (proxHA): Bioactive PCL fiber

meshes (Ø = 9 mm) were thoroughly rinsed in PBS buffer prior to embedding into a hydrogel based on primary oxidized hyaluronic acid (proxHA). Hydrogels were prepared in PBS buffer with a final polymer concentration of 3% w/w. The polymer was dissolved for 3 h at 37 °C, and crosslinked with 1% w/w adipic acid dihydrazide (ADH) solution. For all hydrogels, an equimolar ratio of aldehyde to hydrazide was used. The ADH solution was added to the polymer solution and thoroughly mixed for 5 s. Hydrogel precursor solution (150 µL) was filled into a cylindrical silicon mold (Ø = 12 mm; h = 2 mm), and the gels were allowed to crosslink for 15 min in a petri dish with wet tissues to avoid drying. Afterward, the PCL fiber mesh was placed on top, covered with 150 µL freshly prepared hydrogel precursor solution, and the gels were allowed to crosslink for a further 1.5 h.

The composite specimens were unmolded and rinsed with 2 mL pure HBSS buffer each for 1 h and subsequently incubated with in vitro-derived HNE (+ HNE) or without HNE (- HNE) for 24 h at 37 °C. The supernatant was removed, and the composites were further incubated in pure HBSS to ensure hydrogel dissolution within the following 5 days. Prior to cell seeding, the retrieved fiber meshes were disinfected with 70% EtOH for 30 min and rinsed 4 times with 1x PBS.

Cell Culture Experiments on PCL Meshes: Human mesenchymal stromal cells (hMSCs) were isolated and propagated as previously described[35] from a trabecular bone from the femoral head of patients undergoing total hip arthroplasty at the Orthopedics Department of the University of Würzburg (Germany) with the approval of the Local Ethics Committee of the University of Würzburg and the informed consent of the patients. Briefly, the cells were expanded in propagation medium comprised of Dulbecco's Modified Eagle's medium: Ham's F12 + GlutaMAX-I supplemented with 10% fetal bovine serum (FBS), 100 U mL^{-1} penicillin, 0.1 mg mL^{-1} streptomycin (all Gibco, Life Technologies GmbH, Darmstadt, Germany), and 5 ng mL^{-1} bFGF (Bio Legend, San Diego, CA). For all in vitro experiments, hMSCs up to passage 5 were used. Cells were trypsinized from tissue culture-treated polystyrene (TCPS) flasks and seeded onto non-wovens in a 24-well non-treated culture plate (Corning, New York, USA) using 70.000 cells per well in 1 mL propagation medium. The meshes were fixed onto the plate bottom with a stainless steel annulus. Afterward, the cells were incubated for 24 h at 37 °C in a 5% CO_2, humidified atmosphere.

Quantification of Cell Adhesion and Metabolic Cell Activity on PCL Meshes: hMSC adhesion was examined using the cell proliferation reagent WST-1 (Roche Diagnostics, Mannheim, Germany), which determines metabolic cell activity of the cells. For that, the non-wovens were transferred to fresh well plates and washed once with fresh culture medium. According to the manufacturer's instructions, cells on fiber meshes were incubated in a 1:10 dilution of the WST-1 reagent/propagation medium. After incubation at 37 °C for 30 min, the absorption of the supernatant was measured by means of a Tecan Spark 20M plate reader (Tecan, Crailsheim, Germany) at 450 nm.

Furthermore, the DNA amount of adherent cells was determined using the Quant-iT PicoGreen dsDNA Reagent and Kit (Thermo Fisher Scientific, Waltham (USA)) according to the manufacturer's instruction. Briefly, the specimens were washed twice with 1x PBS, lysed in 0.5% aqueous Thesit solution, and sonicated with a Sonifier W-250D (G. Heinmann, Schwäbisch Gmünd, Germany). The samples were excited at 485 nm and the fluorescence emission intensity was measured at 538 nm on the plate reader.

Scanning Electron Microscopy (SEM): For the examination of hMSC adhesion and morphology, adherent cells were fixed with 6% glutaraldehyde for 15 min, followed by washing twice in ice-cold 1x PBS. Sample dehydration was achieved via incubation in increasing concentrations of ethanol (50%, 70%, 90%, and 100%; twice per concentration, 10 min each). Finally, the constructs were incubated in hexamethyldisilazane twice for 15 min and left to dry overnight in the fume hood. Furthermore, the morphology of electrospun fiber meshes without cells was analyzed directly after the electrospinning process. The SEM samples were coated with a 3 nm thick conductive platinum layer in a Leica EM ACE600 sputtering unit (Leica Microsystems, Wetzlar, Germany) to prevent charging artifacts. An SEM device (Crossbeam 340 FIB-SEM, Carl Zeiss Microscopy GmbH, Oberkochen, Germany) was used for visualization.

Live/Dead Staining: Cell viability was determined by live/dead staining (LIVE/DEAD® Viability/Cytotoxicity Kit, for mammalian cells, Thermo Fisher Scientific Inc., Waltham, USA) according to the manufacturer's instructions. Briefly, 24 h after cell seeding, samples were washed twice with 1x PBS, placed in a 24-well plate and incubated in 500 µL staining solution per well for 30 min in the dark. The solution was aspirated and the samples were washed and stored in 1x PBS. The fluorescence images were immediately recorded with an Axio Imager M1 fluorescence microscope (Carl Zeiss, Jena).

Assessment of In Vitro-Derived HNE Activity: In vitro-derived HNE activity was determined by measuring the release of *para*-nitroanilide (*p*NA) using Cys-Gly-$(Ala)_2$-Pro-Val-p-nitroanilide (CGAAPV-*p*NA) as substrate.

CGAAPV-*p*NA peptide (0.1 mg), dissolved in dry DMSO, was incubated with (+) or without (–) HNE. The absorbance was continuously measured for 180 min at 400 nm using a Tecan Spark 20M plate reader.

Assessment of In Vitro-Derived HNE Diffusion through proxHA Hydrogel: Diffusion of HNE through proxHA hydrogels was determined by measuring the release of *para*-nitroanilide (*p*NA) using CGAAPV-*p*NA as substrate. In detail, CGAAPV-*p*NA peptide (0.12 mg), dissolved in DMSO, was mixed with pure HBSS and stored in the lower compartment (= substrate solution) of a transwell system. The hydrogel precursor solution was prepared as described above and the gel was directly prepared in the insert of the transwell. The volume of the precursor solution was adjusted to form a hydrogel in half of the thickness regarding the composite material described above. To analyze the diffusion of in vitro-derived HNE through the hydrogel, HNE was filled on top of the hydrogel in the insert of the transwell and the well plate was incubated at 37 °C. The absorbance of the storage solution was measured at specific time intervals at 400 nm using a Tecan Spark 20M plate reader. As a positive control, cell inserts without hydrogel but with conditioned HBSS were prepared and measured equally. The absorption intensity of each diffused enzyme solution was related to the positive control (n = 4).

Statistical Analysis: Statistical analyses were performed using Statistica (StatSoft, Oklahoma, USA) by one-way or two-way analysis of variance (ANOVA) followed by Tukey's post hoc test. All data values are presented as mean values ± standard deviation (SD). Results were considered to be significantly different at a p-value below 0.05.

Supporting Information

Supporting Information is available from the Wiley Online Library or from the author.

Acknowledgements

This work was supported by the European Research Council (ERC) (consolidator grant Design2Heal, contract number 617989) and by the German Research Foundation (DFG) ("State Major Instrumentation Programme", funding for the SEM Zeiss Crossbeam 340, INST 105022/58-1 FUGG) and within the Collaborative Research Center TRR225 (project number 326998133-TRR 225, subprojects A02 and A06).

Open access funding enabled and organized by Projekt DEAL.

Conflict of Interest

The authors declare no conflict of interest.

Author Contributions

C.B., T.S., K.S., J.T., and J.G. designed research; C.B. performed research and analyzed data; J.S., J.T. prepared proxHA synthesis; M.B.T. prepared solution electrospun meshes; C.B. prepared the manuscript in consultation with T.S., K.S., J.T. and J.G; J.S. and M.B.T. provided feedback on the manuscript.

Data Availability Statement

Research data are not shared.

Keywords

human neutrophil elastase (HNE), peptide immobilization, polymeric matrix, solution electrospinning

Received: November 30, 2020
Revised: February 10, 2021
Published online: March 9, 2021

[1] a) K. S. Hellmund, B. Koksch, *Front. Chem.* **2019**, *7*, 172; b) F. Xing, L. Li, C. Zhou, C. Long, L. Wu, H. Lei, Q. Kong, Y. Fan, Z. Xiang, X. Zhang, *Stem Cells Int.* **2019**, *2019*, 1.
[2] B. D. Ratner, S. J. Bryant, *Annu. Rev. Biomed. Eng.* **2004**, *6*, 41.
[3] a) N. Huebsch, D. J. Mooney, *Nature* **2009**, *462*, 426; b) S. J. Hollister, *Nat. Mater.* **2005**, *4*, 518.
[4] a) Z. Ma, M. Kotaki, R. Inai, S. Ramakrishna, *Tissue Eng.* **2005**, *11*, 101; b) D. Grafahrend, K.-H. Heffels, M. V. Beer, P. Gasteier, M. Möller, G. Boehm, P. D. Dalton, J. Groll, *Nat. Mater.* **2010**, *10*, 67.
[5] a) A. Rossi, L. Wistlich, K.-H. Heffels, H. Walles, J. Groll, *Adv. Healthcare Mater.* **2016**, *5*, 1939; b) L. Wistlich, J. Kums, A. Rossi, K.-H. Heffels, H. Wajant, J. Groll, *Adv. Funct. Mater.* **2017**, *27*, 1702903.
[6] N. Huettner, T. R. Dargaville, A. Forget, *Trends Biotechnol.* **2018**, *36*, 372.
[7] J. Nicolas, S. Magli, L. Rabbachin, S. Sampaolesi, F. Nicotra, L. Russo, *Biomacromolecules* **2020**, *21*, 1968.
[8] G. S. Hussey, J. L. Dziki, S. F. Badylak, *Nat. Rev. Mater.* **2018**, *3*, 159.
[9] J. M. Anderson, A. Rodriguez, D. T. Chang, *Semin. Immunol.* **2008**, *20*, 86.
[10] E. Mariani, G. Lisignoli, R. M. Borzì, L. Pulsatelli, *Int. J. Mol. Sci.* **2019**, *20*, 636.
[11] K. Prame Kumar, A. J. Nicholls, C. H. Y. Wong, *Cell Tissue Res.* **2018**, *371*, 551.
[12] a) T. A. Wilgus, S. Roy, J. C. McDaniel, *Adv. Wound Care* **2013**, *2*, 379; b) G. S. Selders, A. E. Fetz, M. Z. Radic, G. L. Bowlin, *Regener. Biomater.* **2017**, *4*, 55.
[13] a) B. Korkmaz, T. Moreau, F. Gauthier, *Biochimie* **2008**, *90*, 227; b) D. A. Chistiakov, Y. V. Bobryshev, A. N. Orekhov, *Exp. Mol. Pathol.* **2015**, *99*, 663.
[14] F. Grinnell, M. Zhu, *J. Invest. Dermatol.* **1996**, *106*, 335.
[15] L. W. Heck, W. D. Blackburn, M. H. Irwin, D. R. Abrahamson, *Am J Pathol* **1990**, *136*, 1267.
[16] a) R. Kittelberger, T. J. Neale, K. T. Francky, N. S. Greenhill, G. J. Gibson, *Biochim. Biophys. Acta, Mol. Basis Dis.* **1992**, *1139*, 295; b) W. Kafienah, D. J. Buttle, D. Burnett, A. P. Hollander, *Biochem. J.* **1998**, *330*, 897.
[17] P. Lu, K. Takai, V. M. Weaver, Z. Werb, *Cold Spring Harbor Perspect. Biol.* **2011**, *3*, a005058.
[18] a) N. Bhardwaj, S. C. Kundu, *Biotechnol. Adv.* **2010**, *28*, 325; b) E. S. Place, N. D. Evans, M. M. Stevens, *Nat. Mater.* **2009**, *8*, 457.
[19] a) B. M. Baker, A. O. Gee, N. P. Sheth, G. R. Huffman, B. J. Sennett, T. P. Schaer, R. L. Mauck, *J. Knee Surg.* **2009**, *22*, 45; b) I. C. Bonzani, J. H. George, M. M. Stevens, *Curr. Opin. Chem. Biol.* **2006**, *10*, 568.
[20] P. Zahedi, I. Rezaeian, S.-O. Ranaei-Siadat, S.-H. Jafari, P. Supaphol, *Polym. Adv. Technol.* **2010**, *21*, 77.
[21] S. H. Lim, H. Q. Mao, *Adv. Drug Delivery Rev.* **2009**, *61*, 1084.
[22] D. Grafahrend, K.-H. Heffels, M. Möller, D. Klee, J. Groll, *Macromol. Biosci.* **2010**, *10*, 1022.
[23] J. Salber, S. Grater, M. Harwardt, M. Hofmann, D. Klee, J. Dujic, H. Jinghuan, J. Ding, S. Kippenberger, A. Bernd, J. Groll, J. P. Spatz, M. Moller, *Small* **2007**, *3*, 1023.
[24] J. Bockelmann, K. Klinkhammer, A. von Holst, N. Seiler, A. Faissner, G. A. Brook, D. Klee, J. Mey, *Tissue Eng., Part A* **2011**, *17*, 475.
[25] F. E. Ahmed, B. S. Lalia, R. Hashaikeh, *Desalination* **2015**, *356*, 15.
[26] M. J. Castillo, K. Nakajima, M. Zimmerman, J. C. Powers, *Anal. Biochem.* **1979**, *99*, 53.
[27] a) K. Fujie, Y. Shinguh, N. Inamura, R. Yasumitsu, M. Okamoto, M. Okuhara, *Eur. J. Pharmacol.* **1999**, *374*, 117; b) D. M. Clancy, C. M. Henry, G. P. Sullivan, S. J. Martin, *FEBS J.* **2017**, *284*, 1712.
[28] A. V. Ferreira, I. Perelshtein, N. Perkas, A. Gedanken, J. Cunha, A. Cavaco-Paulo, *Appl. Microbiol. Biotechnol.* **2017**, *101*, 1443.
[29] a) U. Hersel, C. Dahmen, H. Kessler, *Biomaterials* **2003**, *24*, 4385; b) A. L. Dunehoo, M. Anderson, S. Majumdar, N. Kobayashi, C. Berkland, T. J. Siahaan, *J. Pharm. Sci.* **2006**, *95*, 1856.
[30] Z. Shao, X. Zhang, Y. Pi, X. Wang, Z. Jia, J. Zhu, L. Dai, W. Chen, L. Yin, H. Chen, C. Zhou, Y. Ao, *Biomaterials* **2012**, *33*, 3375.
[31] A. G. Karakecili, T. T. Demirtas, C. Satriano, M. Gümüsderelioglu, G. Marletta, *J. Biosci. Bioeng.* **2007**, *104*, 69.
[32] E. A. Kamoun, E.-R. S. Kenawy, X. Chen, *J. Adv. Res.* **2017**, *8*, 217.
[33] M. Weis, J. Shan, M. Kuhlmann, T. Jungst, J. Tessmar, J. Groll, *Gels* **2018**, *4*, 82.
[34] M. E. Lau, D. A. Hunstad, *J. Visualized Exp.* **2013**, 50919.
[35] U. Noth, R. Tuli, A. M. Osyczka, K. G. Danielson, R. S. Tuan, *Tissue Eng.* **2002**, *8*, 131.